

Vortical field amplification and particle acceleration at rippled shocks

F. Fraschetti¹

Departments of Planetary Sciences and Astronomy, University of Arizona, Tucson, AZ, 85721, USA

Abstract

Supernova Remnants (SNRs) shocks are believed to accelerate charged particles and to generate strong turbulence in the post-shock flow. From high-energy observations in the past decade, a magnetic field at SNR shocks largely exceeding the shock-compressed interstellar field has been inferred. We outline how such a field amplification results from a small-scale dynamo process downstream of the shock, providing an explicit expression for the turbulence back-reaction to the fluid whirling. The spatial scale of the X-ray rims and the short time-variability can be obtained by using reasonable parameters for the interstellar turbulence. We show that such a vortical field saturation is faster than the acceleration time of the synchrotron emitting energetic electrons.

Keywords: 85-06

1. Introduction

The origin of cosmic-rays (CRs) still eludes the theoretical and observational efforts in astroparticle physics since their discovery more than a century ago. Space and ground-based experiments have been providing us with a wealth of multi-wavelength observations to identify the source and investigate the mechanism of acceleration in various energy bands. Individual shell-type Supernova Remnant (SNR) shocks accelerate charged particles and are believed to provide a significant fraction of the power sustaining the observed CR spectrum. Moreover, realistic corrugated shocks travelling in the inhomogeneous interstellar space generate turbulence in the compressed post-shock fluid.

The inhomogeneity of the unshocked ISM observed over several scales [2] is expected to deform the shock surface rippling the initial local planarity up to scales many orders of magnitude greater than the thermal ion inertial length. *HST* observations of SN1006 [27] constrain the length-scale of the shock ripples to $10^{16} - 10^{17}$ cm. We focus on the interaction of a non-relativistic SNR rippled shock with the turbulence upstream of the shock, disregarding the contribution of accelerated particles at the shock, as justified later.

From detection of non-thermal X-ray rims [31, 4], rapid time-scale variability of X-ray hot spots [30] and γ -ray emission in extended regions [1], a magnetic field at the shock far exceeding the theoretically predicted shock-compressed field has been inferred. Whether or not such a magnetic field amplification in SNR is to be associated with energetic particles at the shock is still subject of controversy.

Magnetic field amplification might be also relevant to *in situ* measurements of the plasma downstream of the solar-wind ter-

mination shock [8], where fluctuations have been measured of the same order as the mean, or to radio observations of Mpc scale shocks at the edge of galaxy clusters [7]. Strong magnetic fields are also required in Gamma-Ray Bursts (GRB) and Active Galactic Nuclei (AGN) outflows to enable sufficient production of non-thermal radiation. In the ISM magnetic energy density and thermal pressure are typically comparable and both amount to a fraction $10^{-9} - 10^{-7}$ of the total internal energy density (including rest mass). Therefore, a compression by an even ultra-relativistic shock (bulk Lorentz factor ~ 100), cannot produce the fraction $10^{-3} - 10^{-1}$ predicted by GRB phenomenological models of afterglow light curves [25].

The passage of an oblique non-relativistic shock through inhomogeneous medium has been known for longtime to generate vorticity in the downstream flow [18]; in a conducting fluid the turbulent motion at scale l with fluid velocity v_l and local density ρ leads exponentially fast to an amplified magnetic field $B^2 = 4\pi\rho v_l^2$ [22]. The encounter of a shock surface with a density clump, also called Richtmyer-Meshkov (RM) instability [6], has been also extensively investigated in plasma laboratory experiments (see [11] and references therein).

Recent numerical 2D-MHD simulations have shown that such an amplification can be very efficient [16, 17]. Ideal MHD applied to 2D rippled shocks has shown that the ISM turbulence might amplify exponentially fast the upstream magnetic field with a growth rate depending on shock and upstream medium properties [13]. Such an amplification is expected to occur downstream of the blast wave, regardless the presence of shock-accelerated particles. Magnetic field may also be enhanced by field line stretching due to Rayleigh-Taylor (RT) instability [19] at the interface between the ejecta and the interstellar medium, i.e., far downstream of the shock. In contrast with the vortical turbulence, late-time RT turbulence might be affected by the highest energy particle gyrating in the downstream fluid far from the shock [15]. However, RT structures are unlikely to

¹Associated Member to LUTH, Observatoire de Paris, CNRS-UMR8102 and Université Paris VII, 5 Place Jules Janssen, F-92195 Meudon Cédex, France.

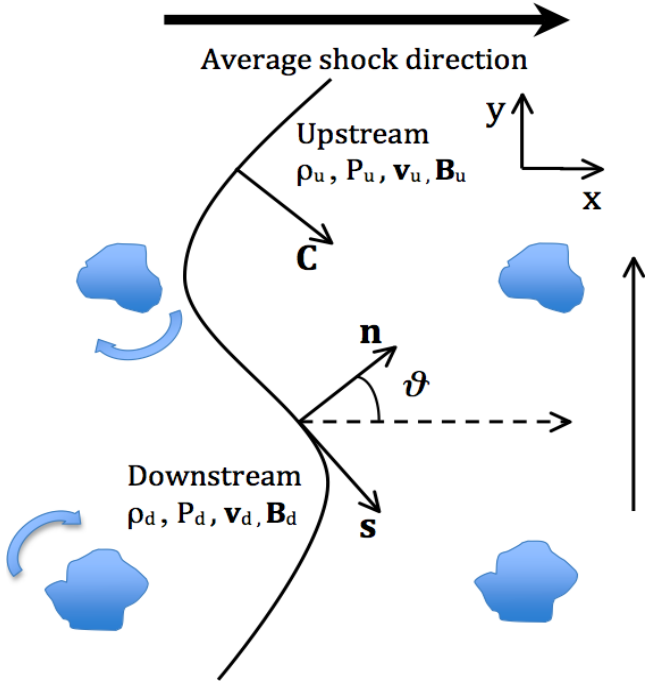


Figure 1: Encounter of a shock surface with density enhancement regions: forward and lagging behind regions are formed that generate vorticity in the downstream fluid.

reach out the blast wave ([15] and references therein) and therefore to interact with vortical turbulence. Thus the dynamo amplification occurring locally behind the shock can be temporally and spatially disentangled from the field line stretching due to RT instability.

Two-dimensional simulations of relativistic shocks [23] show that small-scale dynamo can operate also downstream of the shocks with bulk Lorentz factor of a few unities. This suggests that the dynamo action downstream of shocks might shed light on the energy equipartition at magnetized shocks of AGN and Gamma-Ray Bursts.

2. Macroscopic approach to rippled shock

Constitutive equations - We consider the propagation of a 2D non-relativistic shock front in an inhomogeneous medium. Within the ideal MHD approximation, i.e., with no viscosity or heat conduction, the time evolution of the fluid velocity $\mathbf{v} = \mathbf{v}(x, y, t)$ and the magnetic field $\mathbf{B} = \mathbf{B}(x, y, t)$, is given, for infinitely conductive fluid, by

$$\begin{cases} \partial_t \mathbf{v} + (\mathbf{v} \cdot \nabla) \mathbf{v} + \frac{\nabla P}{\rho} + \frac{1}{4\pi\rho} [\mathbf{B} \times (\nabla \times \mathbf{B})] = 0 \\ \partial_t \mathbf{B} = \nabla \times (\mathbf{v} \times \mathbf{B}) \end{cases} \quad (1)$$

where ρ, P are respectively density and hydrodynamic pressure of the fluid (here $\partial_t = \partial/\partial t$). Note that the current density carried by CRs is here neglected: we aim to identify the growth of the magnetic energy as generated by the vortical motion of the background fluid only. Plasma heating by the shock might reduce the energy deposited in the magnetic turbulence and will be considered in a forthcoming publication.

Vorticity downstream of MHD shock - The vorticity shock-generated is transported along the flow “frozen” into the fluid in the inviscid approximation (Helmholtz-Kelvin theorem). The medium upstream of the shock has $\omega = 0$. The vorticity is calculated downstream at a distance from the shock large enough that the shock is infinitely thin, i.e., the thickness of the shock is much smaller than the local curvature radius at every point of the shock surface.

At a rippled shock the MHD Rankine-Hugoniot jump conditions cannot be applied globally as the directions normal and tangential vary along the shock surface. For a 2D shock propagating at average in the direction x (all quantities are independent on z , see Fig.1), from the velocity field of the flow $\mathbf{v} = (v_x, v_y, 0)$, the vorticity is given by $|\omega| = |\nabla \times \mathbf{v}| = \omega_z$. We use a local natural coordinate system (\hat{n}, \hat{s}) , where $\hat{n} = (\cos\vartheta(t, s), \sin\vartheta(t, s))$ is the coordinate along the normal to the shock surface, $\hat{s} = (\sin\vartheta(t, s), -\cos\vartheta(t, s))$ is the coordinate parallel to the shock surface (Fig.1). We consider a seed-magnetic field upstream uniform and normal to the average direction of motion ($\mathbf{B}_0 = (0, B_0^y, 0)$, or $B_n = B_0 \sin\vartheta$ and $B_s = -B_0 \cos\vartheta$, see Fig.1).

The turbulent field is assumed to be much greater than the shock-compressed field in the downstream flow, in agreement with observations, so that the amplification is efficient at the smallest scales (see Sect. 3). Thus, the vorticity produced downstream of a 2D shock propagating in an inhomogeneous medium with a uniform perpendicular upstream magnetic field (same as for parallel shock [13]) can be recast, neglecting obliqueness, in a simple form (we use $\partial_{x_i} = \partial/\partial x_i$):

$$|\delta\omega_z| = \frac{r-1}{r} \left[\left(\frac{C_r}{\rho} \right)_u \partial_s \rho + \partial_s C_r \right] - \frac{B_n \delta B_s}{4\pi\rho C_r} \partial_s \vartheta, \quad (2)$$

where $r = \rho_d/\rho_u$ is the compression ratio at the shock, C_r is the shock speed relative to the upstream frame, δB_s is the jump across the shock of the magnetic field in the direction locally tangential to the shock surface including the Rankine-Hugoniot compressed seed field and the turbulently amplified field and B_n is the component in the direction locally normal to the shock surface including the unchanged Rankine-Hugoniot and the turbulent components.

Turbulent field amplification - The vortical turbulence described in the previous sub-section exponentially amplifies the total magnetic field. Since the amplification time-scale is of the order of the smallest eddies turnover time [3], the saturation occurs much faster at small-scale [20]. This is the key feature of the small-scale dynamo. The unperturbed field is initially too weak to affect the fluid velocity field and the turbulent field grows exponentially fast, until the magnetic energy produces non-negligible effects on the velocity field and then saturates.

The small-scale dynamo theory predicts that the turbulent field obeys an unbounded exponential amplification at a rate β [20, 21]: $d\varepsilon/dt = 2\beta\varepsilon$, where $\varepsilon = B^2/8\pi\rho$ is the total magnetic energy per unit of mass, including seed and turbulent fields. As shown in [20], the isotropy and homogeneity of the fluid velocity correlation entails the following simple relation between the amplification rate of ε and the vorticity generated downstream of the shock: $\beta \simeq (\pi/3)\delta\omega_z$.

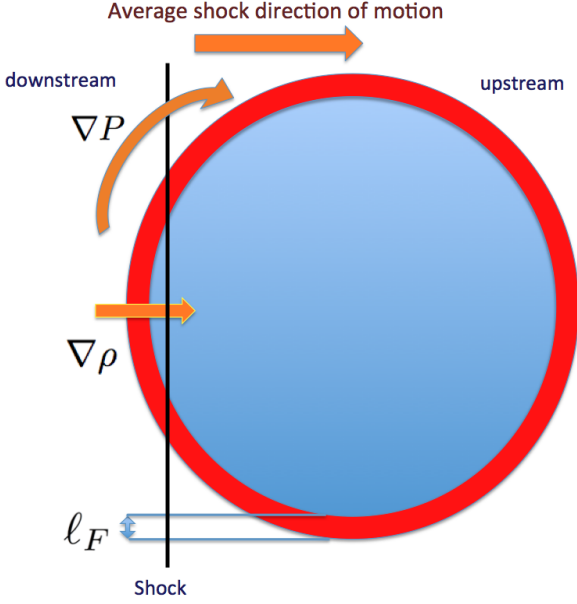


Figure 2: Generation of the baroclinic term of the vorticity at the shock crossing in the condensation layer of thickness ℓ_F .

If we recast Eq.(2) as $|\delta\omega_z| = (3/\pi)(\tau^{-1} - \alpha\varepsilon)$, then ε satisfies

$$\frac{d\varepsilon}{dt} = 2(\tau^{-1} - \alpha\varepsilon)\varepsilon \quad (3)$$

where $\tau^{-1} = \frac{\pi}{3} \frac{r-1}{r} [(C_r/\rho)_u \partial_s \rho + \partial_s C_r]$ is the local growth rate of ε and $\alpha = (2\pi/3) \partial_s \vartheta / C_r$ is the local back-reaction; the initial condition for Eq. (3) is $\varepsilon(0) = \varepsilon_0 = v_A^2/2 = B_0^2/8\pi\rho$. In Eq.(3) we have assumed that the turbulence dominates over B_0 , i.e., $\delta B_s/\sqrt{8\pi\rho} \sim \sqrt{\varepsilon}$ and $B_n/\sqrt{8\pi\rho} \sim \sqrt{\varepsilon}$: the turbulence grows isotropically downstream at the shock curvature scale as a consequence of the isotropy of the flow velocity field [20].

Neglecting the time dependence of τ (the magnetic modes grow slowly for initially weak field [20]), the solution is readily found:

$$\frac{\varepsilon}{\varepsilon_0}(t) = \left(\frac{B}{B_0}\right)^2(t) = \frac{e^{2t/\tau}}{1 - \alpha\tau(1 - e^{2t/\tau})v_A^2/2}, \quad (4)$$

for a uniform average interstellar matter density.

3. Comparison with multiwavelength SNR observations

The growth rate of δB can be approximated as $\tau^{-1} \sim C_r(R_c + \ell_F)/(R_c\ell_F)$, where R_c is the local curvature radius of the shock surface. Thus τ^{-1} increases with shock speed and it depends mainly on hydrodynamic quantities. If $\ell_F \ll R_c$, it holds $\tau \sim \ell_F/C_r$: the amplification saturates faster for smaller ℓ_F .

As the magnetic field strengthens, it reacts to field lines whirling halting the turbulence growth. In more general terms, as the field increases by dynamo action it also releases its tension by unwinding at a rate of order of Alfvén speed: the back-reaction grows with the turbulent field Alfvén speed [20]. The local back-reaction of the field $\alpha \sim \partial_s \vartheta / C_r$ can be estimated by $\alpha \sim \vartheta/(R_c C_r)$.

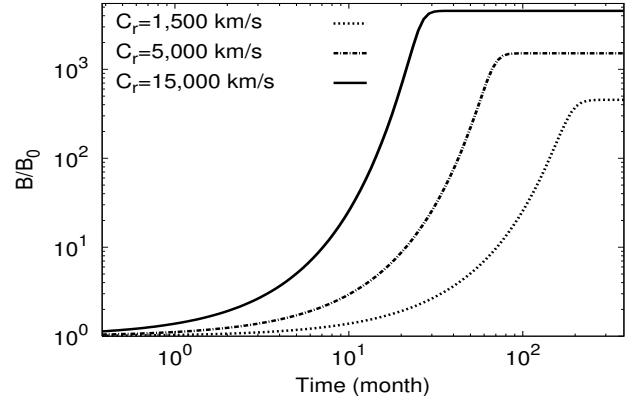


Figure 3: Saturation of the total magnetic field for various shock speed C_r is shown: $C_r = 1,500$ km/s, $C_r = 5,000$ km/s, $C_r = 15,000$ km/s, assuming $R_c = 10^{17}$ cm and $\ell_F = 10^{16}$ cm, that results in $\tau \lesssim \ell_F/C_r \sim 3$ years for $C_r \gtrsim 5,000$ km/s ($\vartheta = 0.1$ rad, $r = 4$ and $v_A = 10^{-4}c$).

Fig.3 depicts the growth of the turbulent field for various shock speeds, assumed constant in time: given an ISM field of the order of $B_0 \sim 3\mu\text{G}$, the turbulent field saturates at $B \sim 1.2 - 3$ mG for $C_r = 1,500 - 5,000$ km/s on the year time-scale. Such a rapid growth of magnetic energy is compatible with X-ray observations of SNRs RXJ1713.7 - 3946 ($C_r < 4,500$ km/s [30]) and Cas A [26] brightness variations detected on year time-scale in small-scale hot spots structures, attributed to synchrotron electron cooling. Using $R_c = 10^{17}$ cm and $\ell_F = 10^{16}$ cm, we find an amplification to $B \sim 3$ mG within 3 years. Such a value of ℓ_F is to be compared with the spatial scale of the *Chandra* RXJ1713.7 - 3946 bright spots, estimated as $\lesssim 0.03$ pc. Similar length ($\sim 10^{14} - 10^{16}$ cm) and time (~ 1 yr) scales are found in simulations of the effects of magnetic field turbulence on the observed synchrotron emission images and spectra in SNRs [9]. Thus, the magnetic energy increase and the X-ray variability might have a time-scale (~ 1 yr) much lower than the SNR hydrodynamic time-scale and might occur in middle-aged, not necessarily young, SNRs (RXJ1713.7 - 3946 age is estimated as 1,600 yr [29]). The high shock speed $C_r \sim 15,000$ km/s in Fig.3 is comparable to observations of the youngest SNR in our galaxy, i.e., 100 years old G1.9 + 0.3 [28]. Thus, a rapid field saturation even up to $B \sim 10$ mG is predicted at SNR shocks within a few months.

4. Constraints on particle acceleration

If the thickness of the density steepening layer at the boundary of the ISM density clumps is identified as the Field length ℓ_F , for typical cold ISM, we can use $\ell_F \approx 3.3 \times 10^{16}$ cm, with an uncertainty depending on ionization and heating/cooling properties [5]. Such an ℓ_F is compatible with the ripple scale inferred by optical observations [27]. Thus, for a typical middle-aged SNR with shock speed $C_r \sim 5,000$ km/s, the growth time-scale of the vortical turbulence is $\tau \approx \ell_F/C_r \approx 6.7 \times 10^7$ s ~ 1.9 yrs.

A simple argument shows that τ is shorter than the typical acceleration time-scale for energetic electrons at the shock, i.e.,

211 τ_{acc} . Modulo a factor of order of unity, $\tau_{acc} \approx \kappa_E/C_r^2$, where the 265
 212 diffusion coefficient κ_E (neglecting its change across the shock) 266
 213 depends on the particle energy and on the magnetic field orien- 267
 214 tation. If the seed magnetic field is parallel to the local shock, 268
 215 normal, the diffusion coefficient governing the electron accel- 270
 216 eration κ_E is necessarily greater than the Bohm diffusion coef- 271
 217 ficient κ_B , corresponding to $\lambda \approx r_g$, where λ is the mean free 272
 218 path of the charged particle and $r_g = pc/eB$ is the particle gyro- 273
 219 radius. The typical energy of an electron emitting synchrotron 275
 220 radiation at 5 keV in an amplified magnetic field $B \sim 100\mu\text{G}$ 276
 221 is $E \sim 50$ TeV. Thus, for an energetic electron diffusing at the 277
 222 shock in the Bohm regime, $\kappa_E = r_g c/3 \approx 3.3 \times 10^{23} E_{13}/B_2$ 279
 223 cm^2/s , where E_{13} is the electron energy in units of 10 TeV and 280
 224 B_2 the magnetic field in the X -ray rim in units of $100\mu\text{G}$. Thus, 281
 225 we obtain $\tau \approx \kappa_E/C_r^2 = 1.9$ years $\approx \tau$. 283
 226 Bohm diffusion, despite largely used in the literature because 284
 227 of the lack of self-consistent diffusion theory in strong turbu- 285
 228 lence, describes transport only for a very limited range of par- 286
 229 ticle energy (see [10, 14]). Since the scattering diffusion coeffi- 287
 230 cient κ_E in most cases is much greater than κ_B , the inferred field 289
 231 amplification might occur on a time-scale much shorter than 290
 232 acceleration time-scale of particles scattering back and forth 291
 233 across the shock. Our simple estimate, derived from the X -ray 292
 234 synchrotron parameters and the inferred strong field, holds re- 293
 235 gardless the location of the emitting region, whether upstream 295
 236 or downstream of the shock. The change of the structure of 296
 237 the turbulence across the shock, due to the anisotropic shock- 298
 238 compression and the vortical amplification downstream shown 299
 239 here, is not expected to modify significantly our estimate of 300
 240 τ_{acc} . 301

241 5. Conclusion

242 By applying first principles to a 2D rippled shock, we have
 243 outlined the derivation of temporal evolution and saturation of
 244 the turbulent magnetic field downstream of the shock, including
 245 the non-linear field back-reaction. We conclude that the satura-
 246 tion of B by small-scale dynamo action depends on the shock
 247 speed, on the thickness of the density steepening layer at the
 248 boundary of the ISM density clumps and on the shock curva-
 249 ture radius, but not on the size of the ISM clumps. Our finding
 250 shows that small-scale dynamo might explain non-thermal X -
 251 ray observations and agrees with the optical upper limit on the
 252 scale of shock ripples. The magnetic field enhancement de-
 253 scribed here occurs faster than acceleration time-scale of syn-
 254 chrotron emitting energetic electrons.

255 *Acknowledgment* – The author thanks ISSI for providing
 256 stimulating environment. The support from NASA through
 257 the Grants NNX10AF24G and NNX11AO64G is gratefully ac-
 258 knowledged.

259 References

- 260 [1] Acciari, V. A. et al. 2011, ApJ Lett., 730, 20
 261 [2] Armstrong, J. W., Rickett, B. J. and Spangler, S. R. 1995, ApJ 443, 209
 262 [3] Balsara, D. S. and Kim, J. 2005, ApJ, 634, 390
 263 [4] Bamba, A., Yamazaki, R., Ueno, M., Koyama, K. 2004, Adv. Space Res.
 264 33, 376

- [5] Begelman, M. C. and McKee, C. F. 1990, ApJ, 358, 375
 [6] Brouillette, M. 2002, Annu. Rev. Fluid Mech, 34, 445
 [7] Brüggem, M., Bykov, A. M., Ryu, D. and Röttgering, H. 2012, Space
 Science Reviews, 166, 187
 [8] Burlaga, L. F., Ness N. J. and Acuña, M.H. 2007, ApJ, 668, 1246
 [9] Bykov, A. M., Uvarov, Y. A. and Ellison, D. C. 2008, ApJ Lett., 689, 133
 [10] Casse, F., Lemoine, M. and Pelletier, G. 2002, Physical Review D, 65,
 023002
 [11] Dimonte, G. and Ramaprabhu, P. 2010, Phys. of Fluids, 22, 014104
 [12] Field, G. B. 1965, ApJ, 142, 531
 [13] Fraschetti, F. 2013, ApJ, 770, 84
 [14] Fraschetti, F. & Giacalone, J. 2012, ApJ, 755, 114
 [15] Fraschetti, F., Teyssier, R., Ballet, J. and Decourchelle, A. 2010, A&A,
 515, A104
 [16] Giacalone, J. and Jokipii, J.R. 2007, ApJ Lett., 663, 41
 [17] Inoue, T., Yamazaki, R., Inutsuka, S. and Fukui, Y. 2012, ApJ, 744, 71
 [18] Ishizuka, T., Hashimoto, Y. and Ono, Y. 1964, Progress of Theoretical
 Physics 32, 207
 [19] Jun, B. I., Norman, M. L. and Stone, J. M. 1995, ApJ, 453, 332
 [20] Kulsrud, R.M. *Plasma Physics for Astrophysics* (Princeton University
 Press, 2005), Chap. 13
 [21] Kulsrud, R.M. and Anderson, S.W. 1992, ApJ, 396, 606
 [22] Landau, L. D. and Lifshitz, E. M. *Electrodynamics of continuous media*
 (Pergamon Press, 1960)
 [23] Mizuno, Y., Pohl, M., Niemiec, J. et al. 2011, ApJ, 726, 62
 [24] Noutsos, A. 2012, Space Science Reviews, 166, 307
 [25] Panaitescu, A. 2005, Monthly Not. Royal Astron. Soc., 363, 1409
 [26] Patnaude, D. J. and Fesen, R. A. 2009, ApJ, 697, 535
 [27] Raymond, J. C., Korreck, K. E., Sedlacek, Q. C., Blair, W. P., Ghavamian,
 P. and Sankrit, R. 2007, ApJ, 659, 1257
 [28] Reynolds, S. P., Borkowski, K. J., Green, D. A., Hwang, U., Harrus, I.
 and Petre, R. 2008, ApJ Lett., 680, 41
 [29] Stephenson, F. R. & Green, D. A. 2002, *Historical Supernovae and their
 remnants*, Oxford Univ. Press
 [30] Uchiyama, Y., Aharonian, F. A., Tanaka, T., Takahashi, T. and Maeda, Y.
 2007, Nature 449, 576
 [31] Vink, J. and Laming, J. M. 2003, ApJ, 584, 758